# Perturbation of the interactions of calmodulin with GRK5 using a natural product chemical probe

Tyler S. Beyett[a,b], Amy E. Fraley[b,c], Emily Labudde[b], Dhabaleswar Patra[d,e], Ryan C. Coleman[f,g], Akito Eguchi[f,g], Alisa Glukhova[b], Qiuyan Chen[d,e], Robert M. Williams[h], Walter J. Koch[f,g], David H. Sherman[b,c,i,j], and John J. G. Tesmer[d,e,1,2]

[a]Program in Chemical Biology, University of Michigan, Ann Arbor, MI 48109; [b]Life Sciences Institute, University of Michigan, Ann Arbor, MI 48109; [c]Department of Medicinal Chemistry, College of Pharmacy, University of Michigan, Ann Arbor, MI 48109; [d]Department of Biological Sciences, Purdue University, West Lafayette, IN 47907; [e]Department of Medicinal Chemistry and Molecular Pharmacology, Purdue University, West Lafayette, IN 47907; [f]Department of Pharmacology, Lewis Katz School of Medicine, Temple University, Philadelphia, PA 19140; [g]Center for Translational Medicine, Lewis Katz School of Medicine, Temple University, Philadelphia, PA 19140; [h]Department of Chemistry, College of Natural Sciences, Colorado State University, Fort Collins, CO 80523; [i]Department of Chemistry, University of Michigan, Ann Arbor, MI 48109; and [j]Department of Microbiology and Immunology, University of Michigan, Ann Arbor, MI 48109

G protein-coupled receptor (GPCR) kinases (GRKs) are responsible for initiating desensitization of activated GPCRs. GRK5 is potently inhibited by the calcium-sensing protein calmodulin (CaM), which leads to nuclear translocation of GRK5 and promotion of cardiac hypertrophy. Herein, we report the architecture of the $Ca^{2+} \cdot CaM$–GRK5 complex determined by small-angle X-ray scattering and negative-stain electron microscopy. $Ca^{2+} \cdot CaM$ binds primarily to the small lobe of the kinase domain of GRK5 near elements critical for receptor interaction and membrane association, thereby inhibiting receptor phosphorylation while activating the kinase for phosphorylation of soluble substrates. To define the role of each lobe of $Ca^{2+} \cdot CaM$, we utilized the natural product malbrancheamide as a chemical probe to show that the C-terminal lobe of $Ca^{2+} \cdot CaM$ regulates membrane binding while the N-terminal lobe regulates receptor phosphorylation and kinase domain activation. In cells, malbrancheamide attenuated GRK5 nuclear translocation and effectively blocked the hypertrophic response, demonstrating the utility of this natural product and its derivatives in probing $Ca^{2+} \cdot CaM$-dependent hypertrophy.

G protein-coupled receptor kinase 5 | calmodulin | malbrancheamide | hypertrophy

**G** protein-coupled receptors (GPCR) are the largest family of cell-surface receptors in humans and regulate numerous physiological processes through the activation of heterotrimeric G proteins, GPCR kinases (GRKs), and arrestins. Mechanisms to attenuate or cease downstream signaling have evolved to maintain proper physiology. The principal desensitization mechanism is initiated by GRKs, which phosphorylate the third intracellular loops or C-terminal tails of active GPCRs. This process facilitates the recruitment of arrestin which sterically occludes G protein binding and promotes receptor internalization (1, 2).

As membrane localization and recognition of activated receptors is critical for efficient receptor desensitization, several regulatory mechanisms have evolved to attenuate GRK activity and prolong receptor activation. The ubiquitous $Ca^{2+}$-binding protein calmodulin (CaM) binds six of the seven GRKs and inhibits both membrane localization and receptor phosphorylation in a $Ca^{2+}$-dependent manner (3–5). The interaction between $Ca^{2+} \cdot CaM$ and GRK5 has been the most studied due to its high affinity ($K_d$ = 8 nM by surface plasmon resonance) and 50-fold greater potency ($IC_{50}$ = 40 to 60 nM toward rhodopsin phosphorylation) compared with other GRKs (3, 4). Coimmunoprecipitation identified N- and C-terminal helical regions of GRK5 (residues 1 to 17 and 552 to 561, respectively) and a stretch of basic residues (residues 20 to 39) near the junction between the kinase and regulator of G protein-signaling homology (RH) domains as regions involved in $Ca^{2+} \cdot CaM$ binding (5, 6).

GRK5 inhibition by $Ca^{2+} \cdot CaM$ is particularly significant because it plays a role in the development of maladaptive cardiac hypertrophy, which affects approximately one third of hypertensive individuals and the majority of individuals following a heart attack (7). After dissociating from membranes, the $Ca^{2+} \cdot CaM$–GRK5 complex translocates to the nucleus where GRK5 phosphorylates histone deacetylase 5 (HDAC5), leading to decreased nuclear levels of HDAC5 and derepression of genes controlled by the transcription factors myocyte enhancer factor-2 (8) and nuclear factor of activated T cells (9, 10). Therefore, blocking the translocation of $Ca^{2+} \cdot CaM$–GRK5 to the nucleus represents a potential therapeutic strategy for ameliorating heart failure (11).

Conflicting models for the $Ca^{2+} \cdot CaM$–GRK5 complex have been proposed. One depicts two separate $Ca^{2+} \cdot CaM$ subunits binding to the distal N- and C-terminal elements of GRK5 in a fashion that would interfere with its membrane binding and receptor phosphorylation (5). Alternatively, recent structures of GRK5 have revealed the N- and C-terminal elements to be in close proximity to one another, thus making it possible for a

## Significance

G protein-coupled receptor (GPCR) kinases (GRKs) are responsible for negatively regulating GPCRs. During periods of cardiac stress, the binding of $Ca^{2+}$ to calmodulin (CaM) promotes nuclear accumulation of GRK5 and maladaptive enlargement of the heart. Here, we use structural analysis and malbrancheamide, a natural product that we show binds to the C-terminal domain of CaM, to reveal the architecture of the CaM–GRK5 complex and the distinct regulatory roles played by each of the domains of CaM in cardiac hypertrophy and GPCR desensitization mediated by GRK5.

single Ca$^{2+}$·CaM to bind both simultaneously (12–14). To better understand the molecular mechanism of inhibition of GRK5 by Ca$^{2+}$·CaM, we used multiple biophysical methods to determine the architecture of the Ca$^{2+}$·CaM–GRK5 complex. Our data are consistent with a single Ca$^{2+}$·CaM molecule binding to multiple elements of the kinase critical for receptor recognition, allosteric activation by phospholipids, and membrane association. We confirm that the binding of Ca$^{2+}$·CaM promotes an active conformation of GRK5 resulting in increased phosphorylation of nonreceptor substrates. The Ca$^{2+}$·CaM–GRK5 interaction was probed with malbrancheamide, a natural product with known activity as a Ca$^{2+}$·CaM inhibitor (15–17). Cocrystallization of malbrancheamide in complex with Ca$^{2+}$·CaM confirmed that the natural product binds to the C-terminal lobe, thus leaving the N-terminal lobe free to interact with other proteins. Malbrancheamide selectively inhibited GRK5 autophosphorylation without affecting substrate phosphorylation and prevented nuclear translocation of GRK5, thereby inhibiting the hypertrophic response in cardiac cells. This method of inhibition allows malbrancheamide to suppress maladaptive Ca$^{2+}$·CaM-stimulated GRK5 membrane dissociation without relieving the benefit of Ca$^{2+}$·CaM-mediated suppression of receptor phosphorylation.

## Results

### A Single Ca$^{2+}$·CaM Binds the RH–Kinase Domain Junction of GRK5.

We first determined the stoichiometry of the Ca$^{2+}$·CaM–GRK5 complex via analytical size exclusion chromatography (SEC) coupled to a multiangle light scattering (MALS) detector. MALS analysis of the peak indicated a molecular weight for the complex of ~90 kDa, indicating a 1:1 stoichiometry (Fig. 1 A and B). To determine the arrangement of Ca$^{2+}$·CaM and GRK5 in complex, we performed SEC–small-angle X-ray scattering (SEC–SAXS) at multiple concentrations (*SI Appendix*, Fig. S1 and Table S1). The higher-concentration samples produced better signal and were used for modeling (*SI Appendix*, Fig. S1 and Table S2). Both samples displayed a plateau in their Porod–Debye plots at a lower q$_{max}$ than their respective Kratky–Debye plots and a normal distribution in their Kratky plots, indicating that the particles do not display a high degree of flexibility (*SI Appendix*, Fig. S2) (18). The Porod exponents of GRK5 and the Ca$^{2+}$·CaM–GRK5 complex were 3.2 and 3.8, respectively, which indicates that the complex is a more compact particle than GRK5 alone.

Unbiased density for GRK5 alone and the Ca$^{2+}$·CaM–GRK5 complex were reconstructed ab initio using the DENSS algorithm (*SI Appendix*, Fig. S3) (19). The crystal structures of Ca$^{2+}$·CaM (PDB 5J03) (20) and GRK5 (PDB 4WNK) (14) with a modeled N-terminal helix (αN) and active site tether (AST) loop from GRK6 (PDB 3NYN) (21) were autodocked into the density (Fig. 1C), and the resulting model agrees with the RAW data ($\chi^2 = 1.07$ by FoXS) (22). The C-terminal binding site (αC) for Ca$^{2+}$·CaM in GRK5, although disordered in prior crystal structures, would be in close proximity to the docked molecule of Ca$^{2+}$·CaM, given the trajectory of the preceding residues in the GRK5 structure, and has been modeled as such. Compared with the density for GRK5 alone (*SI Appendix*, Fig. S3), extra density was observed upon the addition of Ca$^{2+}$·CaM at the junction of the regulator of G protein-signaling homology (RH) and kinase domains (KD) of GRK5. This area is near the N terminus and the basic phospholipid-binding patch, which are known sites of Ca$^{2+}$·CaM binding (23). The positioning of Ca$^{2+}$·CaM in this configuration does not obscure the substrate or ATP-binding pockets, which is consistent with the observation that GRK5 retains catalytic activity toward soluble substrates and autophosphorylation when in complex with Ca$^{2+}$·CaM (3). We next characterized GRK5 and the Ca$^{2+}$·CaM–GRK5 complex by negative-stain electron microscopy and generated reference-free 2D class averages (*SI Appendix*, Fig. S4). Particles of the Ca$^{2+}$·CaM–GRK5 complex revealed additional protein density relative to GRK5 alone in a
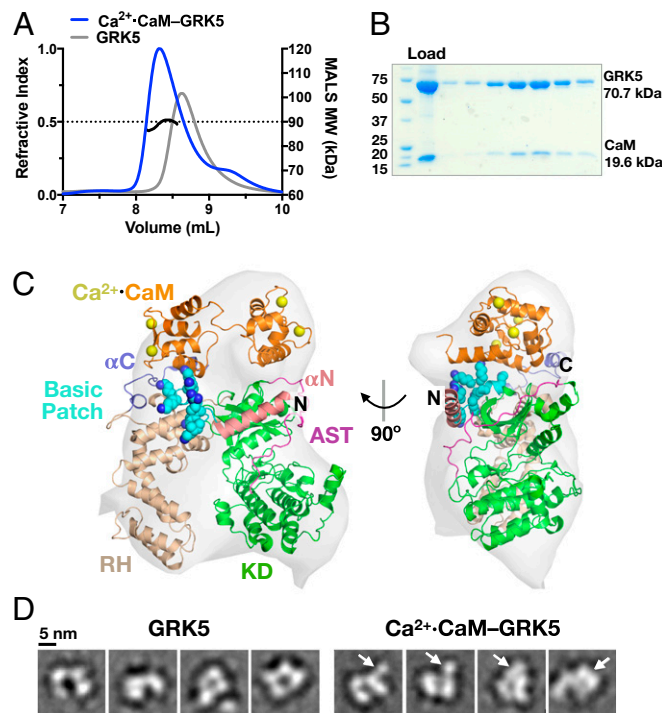


**Fig. 1.** Biophysical characterization of the Ca$^{2+}$·CaM–GRK5 complex. (*A*) Representative chromatograms of GRK5 ± Ca$^{2+}$·CaM (3-fold molar excess) passed over an S200 size exclusion chromatography column. A shift toward a lower elution volume was observed in the presence of Ca$^{2+}$·CaM. MALS determined the molecular weight of the complex to be 90 kDa (solid line inside the peak), the approximate weight of a 1:1 complex (n = 2). The molecular weights of His-tagged GRK5 and CaM are 70.7 and 19.6 kDa, respectively. (*B*) SDS/PAGE analysis of the chromatogram peak corresponding to the Ca$^{2+}$·CaM–GRK5 complex. Both proteins coelute, consistent with complex formation. (*C*) Reconstructed density at 3 σ calculated via DENSS from SEC–SAXS scattering curves of the complex at 10 mg mL$^{-1}$. GRK5 (PDB entry 4WNK) with terminal regions from GRK6 (PDB entry 3NYN) and Ca$^{2+}$·CaM (orange cartoon, PDB entry 5J03) autodocked into the envelope. The regulator of G protein-signaling homology (RH) domain (colored beige), kinase domain (KD; colored green), active-site tether (AST; colored purple), basic phospholipid-binding patch (side-chains shown as spheres), and terminal helices (αN and αC; mauve and purple, respectively) are labeled. The model fits to the RAW SAXS data well ($\chi^2 = 1.07$) as assessed by FoXS. (*D*) Comparison of selected negative-stain class averages of GRK5 alone and the Ca$^{2+}$·CaM–GRK5 complex. Arrows indicate density attributed to Ca$^{2+}$·CaM.

similar position to that indicated in SAXS experiments along a surface spanning the RH domain and N lobe of the kinase domain (Fig. 1D).

### Ca$^{2+}$·CaM Activates GRK5 and Promotes Autophosphorylation.

As previously reported, Ca$^{2+}$·CaM inhibits GRK5-mediated receptor phosphorylation while simultaneously promoting autophosphorylation (Fig. 2A) and enhances phosphorylation of synuclein (4, 24). Our structural analyses are consistent with inhibition of receptor phosphorylation due to Ca$^{2+}$·CaM interacting with regions of GRK5 critical for receptor interaction and/or membrane association. However, autophosphorylation is not simply a consequence of membrane dissociation because Ca$^{2+}$·CaM stimulates autophosphorylation in the absence of membranes or other substrates (Fig. 2B). Although Ca$^{2+}$·CaM inhibits receptor phosphorylation, GRK5 activity toward soluble substrates is enhanced, suggesting that Ca$^{2+}$·CaM binding stabilizes a more active kinase conformation (Fig. 2 C and D). Soluble substrates attenuate autophosphorylation, likely due to competition between the soluble substrate and the C terminus of GRK5. Ca$^{2+}$·CaM is even able to
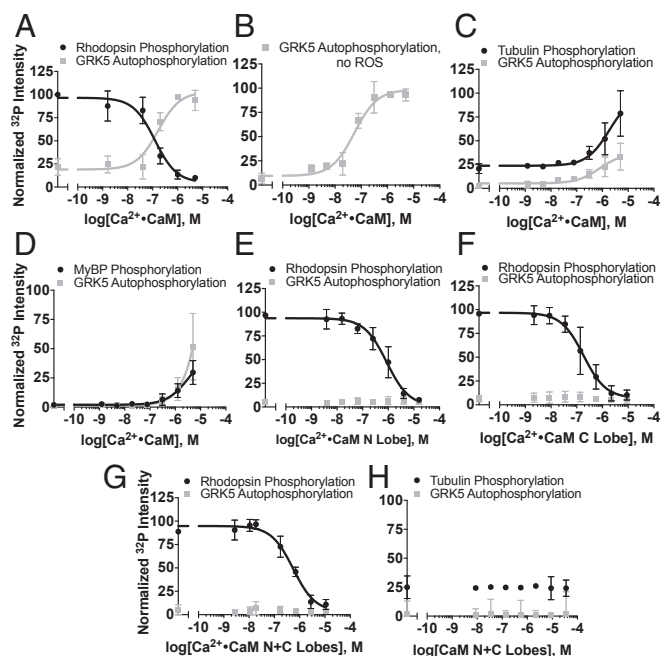
**Fig. 2.** Modulation of substrate phosphorylation by Ca²⁺·CaM. (A) Rhodopsin in rod outer segments (ROS, 5 μM, light-activated) phosphorylation (IC₅₀ = 120 ± 40 nM) and concurrent GRK5 (50 nM) autophosphorylation (EC₅₀ = 170 ± 70 nM) in the presence of Ca²⁺·CaM. (B) Stimulation of GRK5 (50 nM) autophosphorylation by Ca²⁺·CaM (EC₅₀ = 50 ± 20 nM) in the absence of ROS or other substrates. (C) Tubulin (10 μM) phosphorylation in the presence of Ca²⁺·CaM. Decreased potency of concurrent autophosphorylation is likely due to competition between the C terminus of GRK5 and tubulin. (D) Phosphorylation of myelin basic protein (MyBP, 7 μM) presence of Ca²⁺·CaM and concurrent autophosphorylation. Inhibition of rhodopsin phosphorylation by the (E) Ca²⁺·CaM N lobe (IC₅₀ = 860 ± 230 nM), (F) C lobe (IC₅₀ = 180 ± 60 nM), or (G) a 1:1 molar combination of N and C lobes (IC₅₀ = 600 ± 170 nM). (H) Phosphorylation of tubulin is unaffected by the addition of both lobes. All radiometric kinase assays were performed three times and reported as mean ± SD and fit to a sigmoidal dose–response model in GraphPad Prism with the Hill slope constrained to 1.

promote phosphorylation of myelin basic protein (MyBP), which is not phosphorylated by GRK5 in the absence of Ca²⁺·CaM (Fig. 2D), further demonstrating the activating effect of Ca²⁺·CaM. However, because Ca²⁺·CaM is also known to bind MyBP, we cannot exclude the possibility that Ca²⁺·CaM-stimulated phosphorylation of MyBP is due to the formation of a more phosphorylation-prone Ca²⁺·CaM–MyBP complex (25).

To dissect the roles of the individual domains of Ca²⁺·CaM, we studied the effects of its independent N- and C-terminal lobes (residues 1 to 75 and 78 to 149, respectively), which each contain a pair of Ca²⁺-binding EF hand motifs. Both less potently inhibited receptor phosphorylation than full-length Ca²⁺·CaM, consistent with the fact that binding of even a single lobe of Ca²⁺·CaM along the putative membrane interacting surface would interfere with membrane association or receptor binding and diminish receptor phosphorylation (Fig. 2 E and F). Addition of both independent lobes of Ca²⁺·CaM was not sufficient to stimulate autophosphorylation (Fig. 2G) or increase GRK5 activity toward soluble substrates (Fig. 2H), either due to loss of avidity when the lobes are not covalently attached or, more interestingly, if the binding of intact Ca²⁺·CaM binding orients the C terminus of GRK5 in a more optimal way for autophosphorylation.

**Malbrancheamide Binds the C Lobe of Calmodulin and Inhibits Ca²⁺·CaM-Stimulated GRK5 Autophosphorylation.** To dissect how each lobe of CaM is involved in binding the N- and C-terminal binding sites of GRK5, we turned to malbrancheamide, a halogenated

fungal indole alkaloid that antagonizes Ca²⁺·CaM (Fig. 3A) (16) and that has been predicted to bind to the C-terminal lobe (17). We first used isothermal titration calorimetry (ITC) to confirm the binding affinity and stoichiometry of malbrancheamide and the brominated analog isomalbrancheamide D (Fig. 3A and *SI Appendix*, Figs. S5 and S6) (26) for Ca²⁺·CaM. Poor solubility hampered precise measurement of the affinities (Kd), but malbrancheamide and isomalbrancheamide D bound with affinities of 5 ± 1 and 2 ± 1 μM, respectively, consistent with prior reports (16), and bound Ca²⁺·CaM with a 1:1 stoichiometry (Fig. 3A and *SI Appendix*, Figs. S5 and S6).

We next determined crystal structures of Ca²⁺·CaM in complex with malbrancheamide and isomalbrancheamide D. In each complex, the ligand is observed bound with its halogenated indole buried in the hydrophobic pocket of the C lobe (Fig. 3 B–D and *SI Appendix*, Figs. S6 and S7 and Table S3). The halogenated indole is positioned between Leu106, Met125, and Met145, and the C-8 chlorine forms a Cl–π interaction with Phe93. Malbrancheamide buries ~250 Å² of surface area in the hydrophobic pocket (PISA server) (27), consistent with ligands of similar affinity (28). Isomalbrancheamide D is positioned ~0.8 Å deeper in the Ca²⁺·CaM C-lobe hydrophobic pocket, which may explain its slightly higher affinity (*SI Appendix*, Table S3). The N-terminal lobe of Ca²⁺·CaM, however, is free to interact with other proteins (Fig. 3B). Due to limited quantities of isomalbrancheamide D, only malbrancheamide was examined for its ability to modulate the Ca²⁺·CaM–GRK5 interaction. Addition of malbrancheamide to phosphorylation reactions containing Ca²⁺·CaM–GRK5 and rhodopsin inhibited GRK5 autophosphorylation, but did not rescue receptor phosphorylation (Fig. 4A and *SI Appendix*, Fig. S8), consistent with Ca²⁺·CaM being simultaneously bound to malbrancheamide and GRK5. Malbrancheamide had no effect on phosphorylation of the soluble substrate tubulin (Fig. 4B).

**N Lobe of Ca²⁺·CaM Interacts with the N Terminus of GRK5 to Inhibit Receptor Phosphorylation.** To decipher which lobe of CaM is binding to the CaM-binding elements of GRK5, peptides spanning the
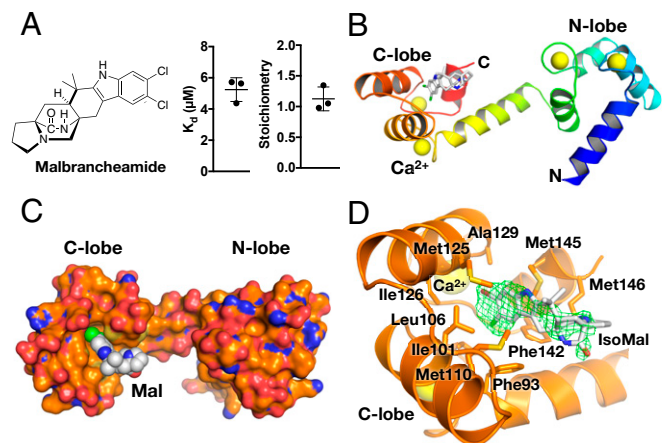


**Fig. 3.** Malbrancheamide binds to the C lobe of Ca²⁺·CaM. (A) Chemical structure of malbrancheamide and ITC-binding results (average ± SD, n = 3). (B) Rainbow ribbon representation of the Ca²⁺·CaM·malbrancheamide structure in a *trans* conformation. Ca²⁺ are shown as yellow spheres (PDB entry 6EEB). (C) Surface representation of Ca²⁺·CaM (orange corresponding to carbon, blue nitrogen, and red oxygen) with malbrancheamide shown as spheres with white carbon atoms, green chlorine. (D) C-lobe hydrophobic pocket with isomalbrancheamide D (IsoMal) bound (bromine colored brown). Green cage represents simulated annealing |Fo| − |Fc| omit density contoured at 2.5 σ. Side-chains making van der Waals contacts with IsoMal are labeled and are similar to those contacting malbrancheamide (*SI Appendix*, Fig. S7). Color scheme is the same as in C.
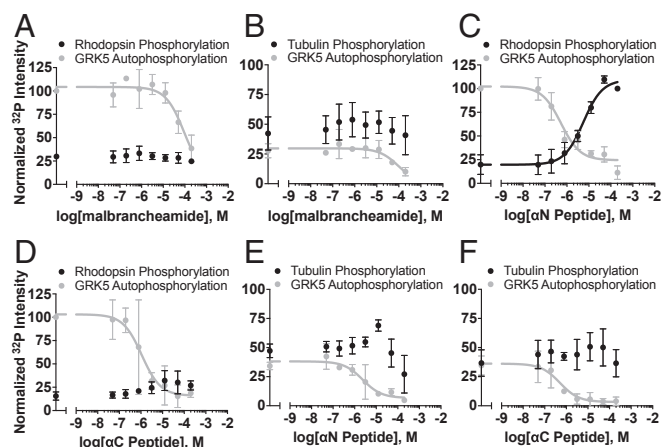
**Fig. 4.** Effects of malbrancheamide and GRK5 peptides on $Ca^{2+}\cdot CaM$ modulation of GRK5 activity. (*A*) Rhodopsin (5 μM, light-activated) phosphorylation in the presence of 500 nM $Ca^{2+}\cdot CaM$ and increasing concentrations of malbrancheamide. In these assays, $Ca^{2+}\cdot CaM$ was preincubated with malbrancheamide before the addition of GRK5. (*B*) Tubulin (5 μM) phosphorylation in the presence of 500 nM $Ca^{2+}\cdot CaM$ and varying concentrations of malbrancheamide. (*C*) Rhodopsin phosphorylation in the presence of 500 nM $Ca^{2+}\cdot CaM$ and varying concentrations of GRK5 αN (residues 2 to 31, $IC_{50,autophosphorylation} = 540 \pm 240$ nM, $EC_{50,rhodopsin} = 5.6 \pm 1.6$ μM) or (*D*) αC (residues 546 to 565, $IC_{50} = 1.1 \pm 0.7$ μM) peptides. (*E*) Tubulin phosphorylation in the presence of 500 nM $Ca^{2+}\cdot CaM$ and varying concentrations of GRK5 αN ($IC_{50} = 2.4 \pm 1.7$ μM) or (*F*) αC peptides ($IC_{50} = 500 \pm 440$ nM). All assays were performed three times and reported as mean ± SD and fit to a sigmoidal dose–response model in GraphPad Prism with the Hill slope constrained to 1.

known $Ca^{2+}\cdot CaM$ binding sites on the termini of GRK5, αN (residues 2 to 31, $K_d = 250$ nM) (*SI Appendix*, Fig. S9) and αC (residues 546 to 565, $K_d = 670$ nM), were evaluated for their ability to disrupt regulation of GRK5 by $Ca^{2+}\cdot CaM$. In the presence of rhodopsin, both peptides inhibited autophosphorylation (Fig. 4 *C* and *D*). However, whereas the addition of the αN peptide rescued receptor phosphorylation, addition of the αC peptide did not, mimicking the effect observed upon addition of malbrancheamide (Fig. 4*D*). Thus, the interaction between the C terminus of GRK5 and the C lobe of $Ca^{2+}\cdot CaM$ is obstructed by the binding of malbrancheamide. Neither peptide affected soluble substrate phosphorylation (Fig. 4 *E* and *F*), although similar inhibition of autophosphorylation was observed in each case. These results indicate that the C lobe of $Ca^{2+}\cdot CaM$ not only binds to the C terminus of GRK5, but is also involved in dictating the autophosphorylation of the GRK5 C terminus.

**Malbrancheamide Inhibits Nuclear Translocation of GRK5 and Prevents Hypertrophy.** We hypothesized that malbrancheamide binding to the C lobe of $Ca^{2+}\cdot CaM$ would allow the C terminus of GRK5 to bind the plasma membrane (Fig. 1*C*) and reduce its nuclear translocation (11). To test this, we first cultured primary neonatal rat cardiac fibroblasts and pretreated cells with 1 μM malbrancheamide or DMSO as a control. This was followed by induction of $Ca^{2+}\cdot CaM$–GRK5-dependent nuclear translocation and accumulation with the GPCR-dependent hypertrophic agonists angiotensin II (AngII) or phenylephrine (PE) (29). Malbrancheamide treatment prevented nuclear accumulation of GRK5 after addition of agonist compared with nonstimulated vehicle-treated controls, as determined by quantitative Western blotting of purified nuclear fractions of cardiac fibroblasts (Fig. 5 *A* and *B*).

In a second set of experiments to confirm malbrancheamide inhibition of GRK5 nuclear accumulation, we examined cardiomyocyte hypertrophy in response to the same agonists (29). Pretreatment of a cardiomyocyte cell line with malbrancheamide

or DMSO as a control was followed with 48 h of PE, AngII, or vehicle treatment, and myocyte hypertrophy was determined by F-actin staining and imaging quantitation of cell area (Fig. 5*C* and *SI Appendix*, Fig. S10). Malbrancheamide blocked cell hypertrophy induced by either PE or AngII. These data are consistent with a mechanism in which malbrancheamide releases the sequestered C terminus of GRK5 from CaM and thereby promotes retention of GRK5 at the plasma membrane in a state that is unable to phosphorylate GPCRs or translocate to the nucleus.

## Discussion

The role of GRK5 in cardiac hypertrophy has stimulated interest in both therapeutic development targeting the kinase and the underlying molecular mechanisms by which this hypertrophy occurs (11). Recent studies have shed light on the role of GRK5 regulation by $Ca^{2+}\cdot CaM$ during GRK5-mediated cardiac hypertrophy (8, 9, 11, 29), a noncanonical activity for the enzyme, but the structural basis of their interaction has not been reported. Here, we present structural and functional data that reveal a single $Ca^{2+}\cdot CaM$ binds to GRK5 in a manner that interferes with both receptor recognition and membrane association while activating the kinase for phosphorylation of soluble substrates that contribute to maladaptive hypertrophy.

Substrates of $Ca^{2+}\cdot CaM$ often contain amphipathic helices with bulky hydrophobic side-chains which anchor the hydrophobic pockets of each lobe of $Ca^{2+}\cdot CaM$ (30, 31). The terminal helices of GRK5 resemble canonical $Ca^{2+}\cdot CaM$ substrates, and thus our model suggests that terminal hydrophobic residues of the αN and αC helices are likely involved in binding to $Ca^{2+}\cdot CaM$ with additional contribution from electrostatic interactions with the acidic helices of $Ca^{2+}\cdot CaM$ with the N-terminal basic patch (Fig. 6). The αN helix has been proposed in some models to dock into the hydrophobic core of activated GPCRs and is well known to be critical for receptor recognition and phosphorylation (32, 33). It is also thought in activated receptor complexes to interact with the kinase domain and stabilize a closed, active conformation (21). Our results suggest that $Ca^{2+}\cdot CaM$ binds to the small lobe of
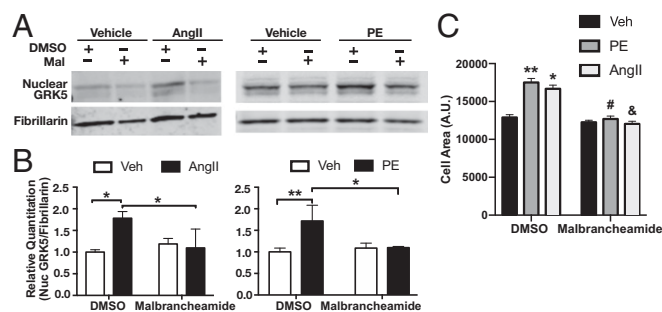


**Fig. 5.** Effects of malbrancheamide on GRK5 nuclear translocation and cardiomyocyte hypertrophy. (*A*) Representative Western blots of nuclear GRK5 following pretreatment with malbrancheamide (Mal) and stimulation with $Ca^{2+}\cdot CaM$ and hypertrophic agonist angiotensin II (AngII) and phenylephrine (PE). Rat neonatal cardiac fibroblasts were pretreated with 1 μM malbrancheamide (or DMSO as control) before treatments with 5 μM AngII or 100 μM PE (or vehicle as control) for 90 min. Nuclear extracts were then prepared and GRK5 was blotted with fibrillarin as a nuclear marker and protein-loading control. (*B*) Quantitation of Western blot results showing significant nuclear localization of GRK5 after AngII (compared with vehicle), which was completely blocked by pretreatment with malbrancheamide (average ± SD, n = 3 biological replicates, two-way ANOVA with Tukey's post hoc correction, *P < 0.05, **P < 0.01). (*C*) Quantitation of myocyte cell area was performed using F-actin stained cells and Image-J software. Three independent experiments were carried out, and 50 to 100 cells per experiment were measured for each included condition. Shown is the average ± SD (*P < 0.05 vs. DMSO vehicle, **P < 0.01 vs. DMSO vehicle, #P < 0.001 vs. DMSO PE, &P < 0.001 vs. DMSO AngII, two-way ANOVA with Tukey's post hoc correction).

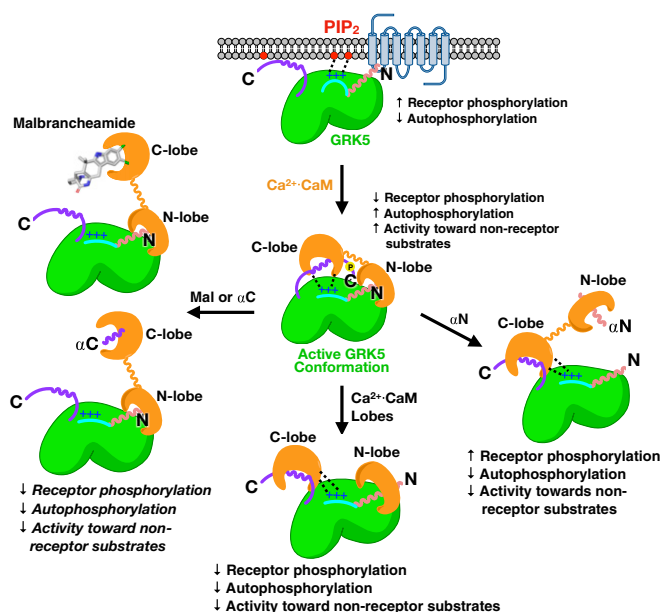**Fig. 6.** Model for lobe-specific regulation of GRK5 by Ca²⁺·CaM. Features critical for receptor docking (αN helix shown as pink wavy line) and membrane association (purple C terminus of GRK5 and the N-terminal basic patch, shown as a blue line with + signs) are sequestered by Ca²⁺·CaM but also stabilize an active conformation of the kinase. Both lobes in the intact protein are required for this activation because simultaneous addition of the individual lobes does not promote an activated state of GRK5. The addition of αN peptide, αC peptide, or malbrancheamide are all able to relieve various aspects of regulation through differential binding to the two lobes of Ca²⁺·CaM.

GRK5 in a manner that sterically hinders GRK5 docking with cognate receptors. A C-terminal amphipathic helix in GRK5 significantly contributes to membrane association (34, 35), and our data further suggest that the GRK5 αC helix is close enough to be sequestered by Ca²⁺·CaM bound via its other lobe to the GRK5 N terminus, thereby also blocking membrane association, which is important for efficient GRK5-mediated phosphorylation of active GPCRs (36).

Although Ca²⁺·CaM potently inhibits receptor phosphorylation, the activity of GRK5 toward soluble substrates is enhanced by three- to fourfold. It was previously reported that Ca²⁺·CaM stimulates phosphorylation of synuclein (24), and this boost in activity clearly extends to other soluble substrates, suggesting that the binding of Ca²⁺·CaM stabilizes an activated conformation of GRK5. Based on the crystal structure of closely related GRK6 in complex with the nucleoside inhibitor sangivamycin (21), the activated state of GRK5 is believed to be stabilized by a network of contacts between the αN helix and the two lobes of the active kinase domain. Because our data provide evidence that Ca²⁺·CaM binds near these elements, stabilization of the αN interaction network likely explains the increase in GRK5 activity toward its soluble substrates. Addition of the isolated lobes of Ca²⁺·CaM, however, did not activate kinase activity at any concentration tested, indicating that full-length Ca²⁺·CaM is required for stabilizing this active conformation, perhaps through improved affinity.

Ca²⁺·CaM-stimulated autophosphorylation of GRK5 has been mapped to noncanonical residues in the extreme C terminus (residues 579 to 590) that, similarly to phosphorylation of this region by protein kinase C (37), further reduces the ability of GRK5 to associate with membranes and thereby could represent a mechanism to prolong both inhibition of receptor phosphorylation and nuclear targeting after Ca²⁺·CaM has dissociated (38).

Cleavage of the helix connecting the two lobes of Ca²⁺·CaM abolished Ca²⁺·CaM-stimulated autophosphorylation, suggesting that intact Ca²⁺·CaM positions the terminal elements of GRK5 in a specific conformation that may enable autophosphorylation *in cis*. Although this is the simplest model, further experiments are needed to exclude the possibility of *trans*-autophosphorylation or a combination of the two. A likely mechanism for this "repositioning" may simply be loss of membrane interactions of the C-terminal region of GRK5 via the binding of Ca²⁺·CaM, which would free this disordered region to instead enter the active site of the kinase domain. However, in the absence of membranes and Ca²⁺·CaM, GRK5 still does not display robust autophosphorylation (Fig. 2B). Thus, it is more likely that Ca²⁺·CaM both redirects the path of the C terminus into the active site while stabilizing an activated conformation of GRK5, leading to enhanced autophosphorylation.

Determination of the roles of the individual lobes of Ca²⁺·CaM was aided by malbrancheamide, a natural product that we show binds solely to the C lobe. This implies that addition of the compound would block the interactions of GRK5 with the C lobe. Indeed, the addition of malbrancheamide or the αC peptide inhibited kinase autophosphorylation, but did not relieve the inhibition of receptor phosphorylation mediated by Ca²⁺·CaM. This is consistent with the C lobe of Ca²⁺·CaM interacting with the C terminus of GRK5, which dissociates the kinase from membranes, whereas the N lobe interacts with the αN helix where it competitively interferes with receptor binding and receptor phosphorylation. It has been previously noted that rhodopsin phosphorylation is similarly inhibited by an antibody that recognizes epitopes in the N terminus of GRK1 without affecting soluble substrate phosphorylation (39). Thus, Ca²⁺·CaM acts as a GRK5 agonist and a mimic of an activated GPCR.

Extraction of GRK5 from the plasma membrane by Ca²⁺·CaM is thought to allow the nuclear localization sequence located in the large lobe of the kinase to promote nuclear translocation of GRK5 and pathological gene activation (34, 40). Malbrancheamide has a defined binding mode that only blocks C-lobe interactions. We show that low μM concentrations of malbrancheamide block nuclear translocation of GRK5 induced by AngII and PE, known hypertrophic agonists that are potent stimulators of nuclear GRK5 accumulation (29). Further, malbrancheamide was also shown to prevent cardiomyocyte hypertrophy induced by AngII and PE, which GRK5 has previously been shown to potentiate (29). Thus, malbrancheamide is an effective chemical probe for studying Ca²⁺·CaM–GRK5-dependent hypertrophic signaling in cells and may facilitate discovery of the specific roles of each lobe of CaM in other complexes. Ca²⁺·CaM is known to play a role in cardiomyocyte hypertrophy induced by other pathways; thus, the specific mechanisms by which malbrancheamide prevents AngII- or PE-induced cellular hypertrophy, either GRK5-dependent or otherwise, require further investigation. For example, previous work has demonstrated the biological activity of malbrancheamide as an inhibitor of Ca²⁺·CaM–phosphodiesterase 1 and Ca²⁺·CaM–myosin light-chain kinase (16, 17), inducing vasorelaxation through cGMP/NO-dependent pathways.

The ability of Ca²⁺·CaM to extract GRK5 from the plasma membrane and activate the kinase against soluble targets highlights the important role Ca²⁺ plays in the regulation of signaling cascades. Allosteric activation of GRKs by Ca²⁺·CaM thus represents an understudied area of physiology. For example, modulation of Ca²⁺ channels by Gβγ subunits in response to GPCR activation is well understood, particularly in the context of neurotransmission (42), but the role of Ca²⁺·CaM-mediated activation of GRKs in feedback mechanisms downstream of such channels has not been studied. Additionally, activation of phospholipase C β and release of Ca²⁺ induced by Gαq-coupled receptors will ultimately lead to formation of Ca²⁺·CaM, which

will prolong GPCR signaling by globally inhibiting GRKs, in particular GRK5. Thus, future studies may reveal novel crosstalk between GPCRs, GRKs, and ion channels and implicate $Ca^{2+} \cdot CaM$–GRK interactions in the development of new pathologies.

## Materials and Methods

Detailed methods and associated references for experiments described herein are available in the *SI Appendix*. The $Ca^{2+} \cdot CaM \cdot$malbrancheamide and isomalbrancheamide D crystal structures and associated diffraction data have been deposited in the Protein Data Bank with the accession codes 6EEB and 6O5G, respectively.

1. J. J. G. Tesmer, Hitchhiking on the heptahelical highway: Structure and function of 7TM receptor complexes. *Nat. Rev. Mol. Cell Biol.* **17**, 439–450 (2016).
2. K. E. Komolov, J. L. Benovic, G protein-coupled receptor kinases: Past, present and future. *Cell. Signal.* **41**, 17–24 (2018).
3. T. T. Chuang, L. Paolucci, A. De Blasi, Inhibition of G protein-coupled receptor kinase subtypes by Ca2+/calmodulin. *J. Biol. Chem.* **271**, 28691–28696 (1996).
4. A. N. Pronin, D. K. Satpaev, V. Z. Slepak, J. L. Benovic, Regulation of G protein-coupled receptor kinases by calmodulin and localization of the calmodulin binding domain. *J. Biol. Chem.* **272**, 18273–18280 (1997).
5. K. Levay, D. K. Satpaev, A. N. Pronin, J. L. Benovic, V. Z. Slepak, Localization of the sites for Ca2+-binding proteins on G protein-coupled receptor kinases. *Biochemistry* **37**, 13650–13659 (1998).
6. L. Iacovelli, M. Sallese, S. Mariggiò, A. de Blasi, Regulation of G-protein-coupled receptor kinase subtypes by calcium sensor proteins. *FASEB J.* **13**, 1–8 (1999).
7. C. Cuspidi, C. Sala, F. Negri, G. Mancia, A. Morganti; Italian Society of Hypertension, Prevalence of left-ventricular hypertrophy in hypertension: An updated review of echocardiographic studies. *J. Hum. Hypertens.* **26**, 343–349 (2012).
8. J. S. Martini et al., Uncovering G protein-coupled receptor kinase-5 as a histone deacetylase kinase in the nucleus of cardiomyocytes. *Proc. Natl. Acad. Sci. U.S.A.* **105**, 12457–12462 (2008).
9. J. E. Hullmann et al., GRK5-mediated exacerbation of pathological cardiac hypertrophy involves facilitation of nuclear NFAT activity. *Circ. Res.* **115**, 976–985 (2014).
10. D. Sorriento et al., The amino-terminal domain of GRK5 inhibits cardiac hypertrophy through the regulation of calcium-calmodulin dependent transcription factors. *Int. J. Mol. Sci.* **19**, E861 (2018).
11. P. Y. Sato, J. K. Chuprun, M. Schwartz, W. J. Koch, The evolving impact of g protein-coupled receptor kinases in cardiac health and disease. *Physiol. Rev.* **95**, 377–404 (2015).
12. T. S. Beyett, S. J. Bandekar, J. J. G. Tesmer, "Molecular basis for targeting, inhibition, and receptor phosphorylation in the G protein-coupled receptor kinase 4 subfamily" in *Methods in Pharmacology and Toxicology*, V. V. Gurevich, E. V. Gurevich, J. J. G. Tesmer, Eds. (G Protein-Coupled Receptor Kinases, Springer, New York, 2016), pp. 59–74.
13. K. E. Komolov, A. Bhardwaj, J. L. Benovic, Atomic structure of GRK5 reveals distinct structural features novel for G protein-coupled receptor kinases. *J. Biol. Chem.* **290**, 20629–20647 (2015).
14. K. T. Homan et al., Crystal structure of G protein-coupled receptor kinase 5 in complex with a rationally designed inhibitor. *J. Biol. Chem.* **290**, 20649–20659 (2015).
15. S. Martínez-Luis, R. Rodríguez, L. Acevedo, Malbrancheamide, a new calmodulin inhibitor from the fungus Malbranchea aurantiaca. *Tetrahedron* **62**, 1817–1822 (2006).
16. M. Figueroa et al., Fluorescence, circular dichroism, NMR, and docking studies of the interaction of the alkaloid malbrancheamide with calmodulin. *J. Enzyme Inhib. Med. Chem.* **26**, 378–385 (2011).
17. M. González-Andrade et al., Insights into molecular interactions between CaM and its inhibitors from molecular dynamics simulations and experimental data. *J. Biomol. Struct. Dyn.* **34**, 78–91 (2016).
18. R. P. Rambo, J. A. Tainer, Characterizing flexible and intrinsically unstructured biological macromolecules by SAS using the Porod-Debye law. *Biopolymers* **95**, 559–571 (2011).
19. T. D. Grant, Ab initio electron density determination directly from solution scattering data. *Nat. Methods* **15**, 191–193 (2018).
20. R. Strulovich, W. S. Tobelaim, B. Attali, J. A. Hirsch, Structural insights into the M-channel proximal C-Terminus/Calmodulin complex. *Biochemistry* **55**, 5353–5365 (2016).
21. C. A. Boguth, P. Singh, C.-C. Huang, J. J. G. Tesmer, Molecular basis for activation of G protein-coupled receptor kinases. *EMBO J.* **29**, 3249–3259 (2010).
22. D. Schneidman-Duhovny, M. Hammel, J. A. Tainer, A. Sali, Accurate SAXS profile computation and its assessment by contrast variation experiments. *Biophys. J.* **105**, 962–974 (2013).
23. D. Svergun, C. Barberato, M. H. Koch, CRYSOL–a program to evaluate X-ray solution scattering of biological macromolecules from atomic coordinates. *J. Appl. Cryst.* **28**, 768–773 (1995).
24. J. A. Pitcher et al., Phosphatidylinositol 4,5-bisphosphate (PIP2)-enhanced G protein-coupled receptor kinase (GRK) activity. Location, structure, and regulation of the PIP2 binding site distinguishes the GRK subfamilies. *J. Biol. Chem.* **271**, 24907–24913 (1996).
25. A. N. Pronin, A. J. Morris, A. Surguchov, J. L. Benovic, Synucleins are a novel class of substrates for G protein-coupled receptor kinases. *J. Biol. Chem.* **275**, 26515–26522 (2000).
26. J. M. Boggs, Myelin basic protein: A multifunctional protein. *Cell. Mol. Life Sci.* **63**, 1945–1961 (2006).
27. A. E. Fraley et al., Function and structure of MalA/MalA′, iterative halogenases for late-stage C-H functionalization of indole alkaloids. *J. Am. Chem. Soc.* **139**, 12060–12068 (2017).
28. E. Krissinel, K. Henrick, Inference of macromolecular assemblies from crystalline state. *J. Mol. Biol.* **372**, 774–797 (2007).
29. H. V. Waldschmidt et al., Structure-based design, synthesis, and biological evaluation of highly selective and potent G protein-coupled receptor kinase 2 inhibitors. *J. Med. Chem.* **59**, 3793–3807 (2016).
30. J. I. Gold et al., Nuclear translocation of cardiac G protein-Coupled Receptor kinase 5 downstream of select Gq-activating hypertrophic ligands is a calmodulin-dependent process. *PLoS One* **8**, e57324 (2013).
31. P. Kursula, The many structural faces of calmodulin: A multitasking molecular jack-knife. *Amino Acids* **46**, 2295–2304 (2014).
32. S. Bhattacharya, C. G. Bunick, W. J. Chazin, Target selectivity in EF-hand calcium binding proteins. *Biochim. Biophys. Acta* **1742**, 69–79 (2004).
33. C.-C. Huang, J. J. G. Tesmer, Recognition in the face of diversity: Interactions of heterotrimeric G proteins and G protein-coupled receptor (GPCR) kinases with activated GPCRs. *J. Biol. Chem.* **286**, 7715–7721 (2011).
34. C. S. Pao, B. L. Barker, J. L. Benovic, Role of the amino terminus of G protein-coupled receptor kinase 2 in receptor phosphorylation. *Biochemistry* **48**, 7325–7333 (2009).
35. M. M. Thiyagarajan et al., A predicted amphipathic helix mediates plasma membrane localization of GRK5. *J. Biol. Chem.* **279**, 17989–17995 (2004).
36. A. N. Pronin, C. V. Carman, J. L. Benovic, Structure-function analysis of G protein-coupled receptor kinase-5. Role of the carboxyl terminus in kinase regulation. *J. Biol. Chem.* **273**, 31510–31518 (1998).
37. P. Yang, A. Glukhova, J. J. G. Tesmer, Z. Chen, Membrane orientation and binding determinants of G protein-coupled receptor kinase 5 as assessed by combined vibrational spectroscopic studies. *PLoS One* **8**, e82072–e11 (2013).
38. A. N. Pronin, J. L. Benovic, Regulation of the G protein-coupled receptor kinase GRK5 by protein kinase C. *J. Biol. Chem.* **272**, 3806–3812 (1997).
39. R. B. Penn, A. N. Pronin, J. L. Benovic, Regulation of G protein-coupled receptor kinases. *Trends Cardiovasc. Med.* **10**, 81–89 (2000).
40. K. Palczewski, J. Buczyłko, L. Lebioda, J. W. Crabb, A. S. Polans, Identification of the N-terminal region in rhodopsin kinase involved in its interaction with rhodopsin. *J. Biol. Chem.* **268**, 6004–6013 (1993).
41. L. R. Johnson, M. G. H. Scott, J. A. Pitcher, G protein-coupled receptor kinase 5 contains a DNA-binding nuclear localization sequence. *Mol. Cell. Biol.* **24**, 10169–10179 (2004).
42. G. W. Zamponi, K. P. M. Currie, Regulation of Ca(V)2 calcium channels by G protein coupled receptors. *Biochim. Biophys. Acta* **1828**, 1629–1643 (2013).